Molecular Beam Epitaxy

M. B. Panish

Summary. Molecular beam epitaxy is an ultrahigh vacuum technique for growing very thin epitaxial layers of semiconductor crystals. Because it is inherently a slow growth process, extreme dimensional control over both major compositional variations and impurity incorporation can be achieved. The result is that it has been possible, with one combination of lattice-matched semiconductors, GaAs and $Al_xGa_{1-x}As$, to demonstrate a large variety of novel single-crystal structures. These results have important implications for fundamental studies of the physics of thin-layered structures and for the development of new semiconductor electronic and optoelectronic devices.

The advances in solid-state device technology that have taken place since the invention of the transistor have required constant improvements in methods for preparing and processing semiconductors with precise dimensional and compositional constraints. In addition to spectacular growth in the technology of silicon for integrated circuits with increasingly larger densities of devices and functions, there has been steady progress in electronics technology into optical and microwave frequencies that has directed interest to several compound semiconductors. These are usually either binary compounds of one of the group III elements Al, Ga, and In and one of the group V elements P, As, and Sb, or crystalline solid solutions of the binary compounds such as $Al_xGa_{1-x}As$ or $Ga_xIn_{1-x}P_yAs_{1-y}$ with $0 \leq x,y \leq 1$.

The III-V semiconductors have the same gross electronic bonding structure as the better known semiconductors Si and Ge; but because of differences in the detailed nature of that structure, they are sometimes more useful for microwave devices and always more useful as light-emitting devices. In addition, the ability of III-V compounds to form solid solutions means that abrupt transitions in such properties as the energy of the forbidden energy gap and the refractive index can be achieved by compositional changes. For some combinations of these semiconductors, most notably GaAs and $Al_xGa_{1-x}As$, or InP and $Ga_xIn_{1-x}P_yAs_{1-y}$ with the correct ratio of x to y, the size of the crystal lattice can be kept virtually unchanged in spite of the compositional variations, so that changes in important electrical and optical properties can be achieved in very small regions of the crystal without seriously perturbing the crystal structure.

Most of the binary III-V compounds are manufactured as large single-crystal ingots that are sliced into wafers to be used for device fabrication. Frequently, in order to capitalize on the versatility of the III-V semiconductors for solid-state devices, these single-crystal wafers are used as substrates for the subsequent growth of very thin layers of the same or other III-V compounds having the desired electronic or optical properties. This must be done in such a way as to continue, in the grown layer, the crystal structure of the substrate. Such crystal growth, in which the substrate determines the crystallinity and orientation of the grown layer, is called epitaxy, and a variety of epitaxial growth techniques have been developed. The most common of these are vapor phase epitaxy (VPE) and liquid phase epitaxy (LPE). The former utilizes a heated stream of gaseous elements or compounds that interact at the surface of the substrate to form the crystalline layer. In the latter the same end is accomplished by cooling a heated metallic solution saturated with the components needed to grow the layer, while that solution is in contact with the substrate.

In addition to VPE and LPE, vacuum epitaxy has been studied. Günther (*1, 2*) showed in 1958 that thin films of polycrystalline III-V compounds could be grown when the elements comprising the semiconductor were evaporated in a vacuum system with heated walls onto a heated substrate material. In 1966 Steinberg and Scruggs (*3*), using a glass bell jar vacuum system without hot walls, grew epitaxial GaAs onto a heated NaCl single-crystal substrate. Then in 1968 Davey and Pankey (*4*) showed that by using a heated vacuum system with a sufficiently high ambient arsenic pressure, epitaxial GaAs could be grown when a beam of gallium atoms impinged on a heated single-crystal GaAs substrate surface. In the same year Arthur (*5*), using a metal vacuum system that did not have heated walls, impinged beams of both gallium atoms and arsenic molecules onto a heated GaAs substrate wafer and obtained epitaxial growth. The technique that is now generally called molecular beam epitaxy (MBE) derives directly from Arthur's work. His use of a cool-wall, all-metal vacuum system; impinging beams of all components; cryopaneling to yield some beam collimation and to reduce radiative heating of the vacuum system walls by the heated beam sources; and fast pumping techniques to maintain ultrahigh vacuum eventually yielded the cleanliness of the ultrahigh vacuum that now permits vacuum epitaxy of high-quality semiconductor material.

There has been a vigorous effort over the past decade to demonstrate MBE of semiconductor materials useful for semiconductor devices. Much of the credit for bringing this technology to its present state of maturity must be given to Cho (*6, 7*), who used GaAs and $Al_xGa_{1-x}As$ as prototype materials in most of his work. There is now a rather extensive literature on MBE as it has become the subject of research at many laboratories; detailed discussions and bibliographies are given in (*6–9*).

The work of the past few years has clearly demonstrated that MBE is an extraordinarily versatile epitaxy technique that is applicable to a variety of conventional microwave and optoelectronic devices. In addition, because of the extreme dimensional control with MBE, it is possible to build essentially new crystals with periodicities not available in nature and to prepare structures whose properties depend on confinement of holes and electrons to crystalline regions so small that quantum confinement effects become important.

The author is head of the Materials Science Research Department, Bell Laboratories, Murray Hill, New Jersey 07974.

0036-8075/80/0523-0916$01.75/0

Molecular beam epitaxy is, in principle, applicable to the growth of epitaxial layers of a variety of compound semiconductors, and experimental studies of MBE of many different materials have been done or are under way in a number of laboratories. Particularly notable are the studies of InP on InP (*10, 11*), $Ga_xIn_{1-x}As$ on InP (*12*), InAs and GaSb ultrathin layered structures (*13*), Si on Si (*14, 15*) and on sapphire (*16*), and IV-VI compounds (*17*). The MBE efforts on InP and $Ga_xIn_{1-x}P$ on InP and other III-V compounds yield light-emitting devices and detectors at a variety of wavelengths, mostly in the near infrared. The studies of IV-VI compounds do the same for devices for the far infrared. The work with silicon provides an added degree of freedom in doping control and shows promise for higher quality Si on sapphire (SOS) than is now commonly achieved with chemical vapor deposition. In spite of the great variety of MBE work on other materials, most MBE studies to date have been done with GaAs and $Al_xGa_{1-x}As$. For that reason the discussions presented in this article deal only with those semiconductors, which may be considered prototypes, at least for epitaxy of structures of other III-V compounds.

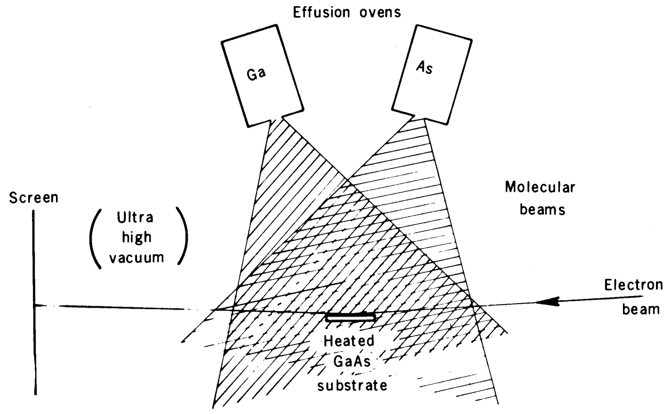

Fig. 1. Schematic representation of a molecular beam epitaxy system.

The Molecular Beam Epitaxy Process

Reduced to its essentials, a system for MBE of GaAs consists of an ultrahigh vacuum system containing sources for atomic or molecular beams of Ga and As and a heated substrate wafer, as illustrated very schematically in Fig. 1. The beam sources are usually containers for the liquid Ga or solid As. They have an orifice that faces the substrate wafer. When the container, or effusion oven as it is usually called, is heated, atoms of Ga or molecules of arsenic effuse from the orifice. The effusing species constitute a beam in which the mean free path is large compared to the distance between the oven orifice and the substrate wafer. If the orifice diameter is small compared to the mean free path of the gaseous components inside the effusion oven, the flux of Ga or As_4 at the target wafer may readily be shown to depend on the partial pressure of the species within the oven, the distance from orifice to substrate, the temperature, the species molecular weight, and the orifice area. Additional ovens, not shown in Fig. 1, may be used to generate a beam of Al, for the growth of $Al_xGa_{1-x}As$, and to generate beams of impurity elements that can be used to make the epitaxial semiconductor *n* or *p* type. Most current MBE systems have about six effusion ovens. The beams may be shut off with shutters interposed between the substrate and the oven orifice, or the beam intensity may be varied by varying the oven temperature. Also illustrated in Fig. 1 is an electron beam that impinges, at a glancing angle, on the growing surface of the crystal for in situ evaluation of surface morphology.

The successful use of MBE for epitaxy of GaAs, $Al_xGa_{1-x}As$, and other III-V compounds is a direct consequence of the behavior of group III atoms and group V molecules on striking the heated substrate surface. Arthur (*5*) showed for GaAs—and it is true for other III-V compounds—that there is a range of substrate temperatures over which virtually all of the group III element adsorbs on the surface. This holds for the entire usual temperature range of 450° to 650°C for the growth of GaAs. The surface lifetime of Ga on GaAs is greater than about 10 seconds, while the arsenic molecules desorb rapidly from a heated GaAs surface unless adsorbed Ga is present. In the latter case the surface lifetime of As increases as it bonds to the Ga. It decreases again when the excess Ga is consumed. The result of this is that one As atom remains on the surface for each Ga atom provided in the Ga beam. For the growth of GaAs the 1 : 1 ratio of Ga to As is maintained in the growing layer simply by having the As_4 flux be greater than the Ga flux. For epitaxy of $Al_xGa_{1-x}As$ the ratio of Al to Ga atoms in the solid is simply the ratio of the atom flux of each during growth, while the ratio of total group III (Al plus Ga) to As atoms in the solid is unity.

Achievement of high crystalline and semiconductor quality of the epitaxial layers also requires that clean ultrahigh vacuum conditions be maintained and that the substrate temperature be sufficiently high that the atoms adsorbing on the surface are mobile enough to migrate to the proper crystal sites. For GaAs, growth usually takes place with a substrate temperature above 450 °C, and for $Al_xGa_{1-x}As$ the temperature is usually above 550 ° or even 600 °C.

Electron Diffraction and Surface Morphology

Molecular beam epitaxy is unique among crystal growth techniques in that it is possible to examine the crystal surface in some detail during the growth process. The electron beam shown in Fig. 1 is diffracted by the regular array of atoms that constitute the crystal structure near or at the surface of the crystal much as light is diffracted by a grating. The diffraction pattern of the electrons yields information about the arrangement of the atoms on the growing crystal surface. If the surface is microscopically rough, the diffraction pattern will be characteristic of the three-dimensional crystal since the beam must penetrate protuberances on the surface. If it is almost smooth on an atomic scale, the diffraction pattern will show the characteristic two-dimensional spacing of the atoms on that surface. This is illustrated in Fig. 2 from a study by Cho (*18*). A set of electron diffraction patterns of a {100} GaAs surface is shown in various stages of MBE growth, with associated electron micrographs showing the morphology of the surface. In Fig. 2a the spotted pattern is for the highly polished, but still microscopically rough starting crystal. The spots result from diffraction from the three-dimensional crystal lattice as the electron beam penetrates the protuberances on the atomically rough surface. Figure 2b shows that after average growth of 150 angstroms the surface is smoother and the diffraction pattern is streaking. The streaked pattern shows the relaxation of one dimension in the diffraction as the electron beam is diffracted more by atoms on the surface than by atoms in the bulk. A new diffraction streak halfway between the main peaks shows that the surface atoms have a unit cell size twice that of the atoms in the bulk. Figure 2c shows that after growth of 1 micrometer the surface is smooth and the diffraction pattern fully streaked. Thus the examination of the electron diffraction pattern during growth of the epitaxial layer yields information about the microscopic smoothness of the crystal surface, and demonstrates that during MBE the microscopic smoothness can be improved over that obtainable with mechanical and chemical polishing.

Impurity Incorporation and Profiling

When some impurity elements (dopants) that have either more or fewer valence electrons than are needed for bonding are incorporated into the semiconductor, it becomes either *n* or *p* type. The impurity atoms in the *n*-type semiconductor have donated electrons that are mobile current carriers and occupy energy states in the conduction band. The impurity atoms in the *p*-type semiconductor have removed electrons from the valence band, leaving behind mobile, positively charged "holes." For the semiconductor to be useful for most solid-state devices, the concentrations of carriers in the *n*- and *p*-type regions must usually be precisely controlled. The quantity of impurity is typically much less than 10^{-5} atom fraction, and in a given structure it is often useful to be able to vary the impurity profile as a function of depth into the crystal so that the conductivity type and profile may be tailored to the device requirements.

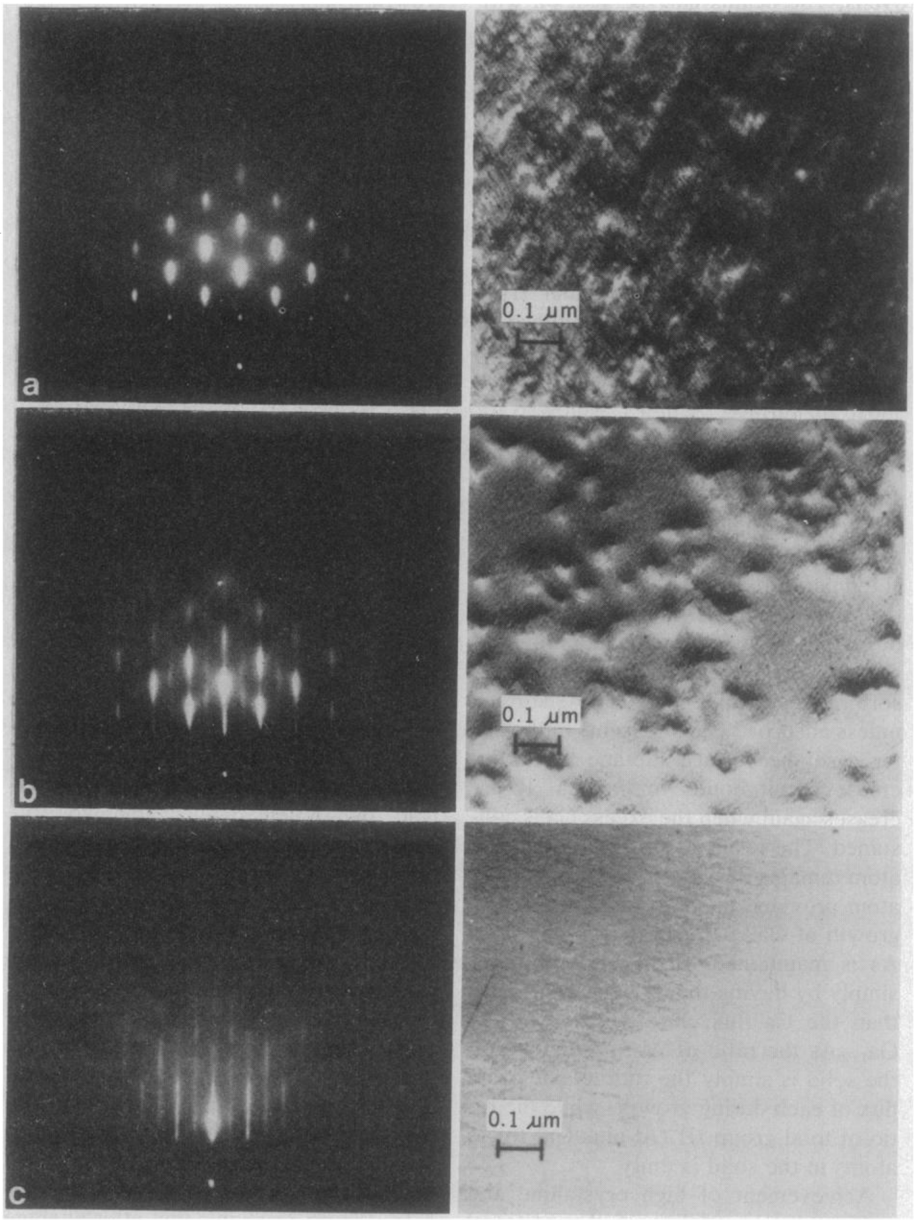

Fig. 2. Reflection electron diffraction patterns (40 kiloelectron volts, $\bar{1}10$ azimuth) and electron micrographs of replicas of the same GaAs surface (*18*). (a) Polish-etched GaAs after heating in a vacuum for 5 minutes. (b) Same after 150 Å of GaAs was deposited by MBE. (c) Same after 1 µm of GaAs was deposited by MBE.

Conventional epitaxy techniques provide only limited control over doping profiles, usually permitting only a fixed or a slowly varying level of impurity in a given layer. Frequently, impurity atoms are diffused or ion-implanted into the surface of a semiconductor. These methods, which are technologically very important, yield a very restricted range of impurity profiles, usually involving either a concentration that decreases monotonically into the crystal or a single peaked distribution.

Because MBE is a slow growth process, layer thicknesses typically increase by 1 µm per hour, and it is possible by varying impurity effusion oven temperatures or by the use of shutters to arbitrarily vary the impurity concentration as a function of depth. This is illustrated (*19*) for Ge added to GaAs in Fig. 3. Three rectangular pulses of Ge in the 1-µm-thick GaAs epitaxial layer yield electron concentrations shown by the dashed curve. The electron concentration profile is, in fact, what would be expected for rectangular impurity profiles. Thus MBE can yield the most abrupt electron concentration profile possible and also all gradations away from that limit. The ability to obtain such arbitrary doping profile control with MBE has been used for the preparation of a number of solid-state devices. These include hyperabrupt varactor diodes that require an exponential doping profile with depth (*20*); IMPATT (impact ionization avalanche transit time) diodes of the so-called low-high-low variety (*21*) that require a 1000-Å-thick doping spike in which the impurity concentration increases by a factor of 10; state-of-the-art field-effect transistors requiring precision doping control in a layer only several thousand angstroms thick (*22*); and state-of-the-art microwave mixer diodes for low-temperature, low-noise operation (*23*). The latter require a very abrupt transition from highly to lightly doped material and are used mostly for radio astronomy.

All of the applications of MBE described above utilize conventional doping levels in the range of about 10^{16} to 10^{18} impurity atoms per cubic centimeter. In addition, it is possible with MBE to achieve doping levels around 5×10^{19} cm^{-3} for both *n*- and *p*-type dopants (Sn and Be) in GaAs and to use oxygen as a dopant for $Al_xGa_{1-x}As$ to render it semi-insulating. The former permits the application of high-quality metal ohmic contacts either in situ by evaporation (*24*, *25*) or out of the MBE system by electroplating, without subsequent heating. The oxygen-doped $Al_xGa_{1-x}As$ has been found to prevent surface leakage of current due to recombination of carriers at GaAs surfaces (*26*). Such passivation provides hope for a metal-insulator-semiconductor technology with GaAs. In addition, since it is an epitaxial part of the crystal structure, the oxygen-doped $Al_xGa_{1-x}As$ provides the solid-state device designer with a new degree of freedom, the possibility of designing devices incorporating lattice-matched semi-insulating regions into the single-crystal device structure.

Heterostructures

Single-crystal multilayered structures having component layers that differ in composition but are lattice-matched form the basis for semiconductor devices in which both light and current carriers (holes and electrons) can be manipulated. The double-heterostructure (DH) laser (*27*) is perhaps one of the best illustrations of these devices. It also provided one of the earliest motivations for MBE studies at Bell Laboratories.

The GaAs-$Al_xGa_{1-x}As$ DH laser in its simplest version is a small rectangular single-crystal parallelepiped consisting of an *n*-type GaAs substrate with at least three layers—*n*-$Al_xGa_{1-x}As$, *p*-GaAs, and *p*-$Al_xGa_{1-x}As$—grown epitaxially onto it as illustrated in Fig. 4, a and b. The alignment of the conduction and valence bands of the composite structure, when forward-biased (*n*-side negative) with a voltage of about the width of the GaAs energy gap, is shown schematically in Fig. 4c. As the result of forward bias, electrons are injected into the conduction band of the *p*-GaAs layer, where they recombine with the majority holes and emit radiation with approximately the energy of the GaAs energy gap, $E_{g_{GaAs}}$. Note in Fig. 4c that at the heterojunction there are potential barriers that prevent holes (e^+) and electrons (e^-) from diffusing beyond the GaAs region. The injected electrical carriers are then confined to the GaAs layer. In addition, because GaAs has a higher refractive index than $Al_xGa_{1-x}As$, the $Al_xGa_{1-x}As$-GaAs-$Al_xGa_{1-x}As$ three-layer sandwich is a waveguide so that the generated light tends to be confined to the GaAs layer. The cleaved ends of the parallelepiped act as partial mirrors. Thus, light of energy approximately $E_{g_{GaAs}}$ is generated by an electronic transition in a waveguide within a Fabry-Perot cavity formed by the mirrors. With a sufficiently high current through the device, stimulated emission and lasing result.

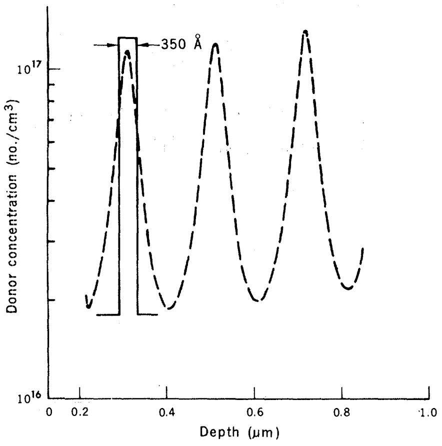

Fig. 3. A periodic doping profile of Ge in GaAs (*19*). The solid curve shows the Ge profile for one peak as estimated from the growth conditions. The dashed curve shows the measured electron distribution in the sample containing three such Ge pulses above a background level.

The DH laser provides an excellent illustration of how heterostructures are used to manipulate light and electrical carriers in a single solid-state device. A variety of other heterostructure devices have also been fabricated. These include optical modulators, optical switches, waveguides, and couplers, all utilizing combinations of GaAs and $Al_xGa_{1-x}As$ layers. There is a growing technology, mostly in optical communications, that utilizes heterostructure lasers as discrete devices. The multilayered wafers used for fabrication of these lasers are at present most often grown by LPE. Because of difficulties in obtaining growth sufficiently free of contamination, the MBE technique has only recently been used to demonstrate high-quality lasers. These lasers have had current densities for the onset of lasing that were comparable to or even lower than those of comparable lasers made with LPE wafers (*28*, *29*). In addition, the properties of many such lasers selected from various areas of several large wafers demonstrated a degree of uniformity that is clearly much better than has been achieved by liquid epitaxy. This achievement is important, not only for the eventual fabrication of discrete devices more reproducibly than has been possible with LPE, but also because the use of integrated electrooptic circuits may become desirable.

Integrated electrooptic circuits made possible by MBE would incorporate not

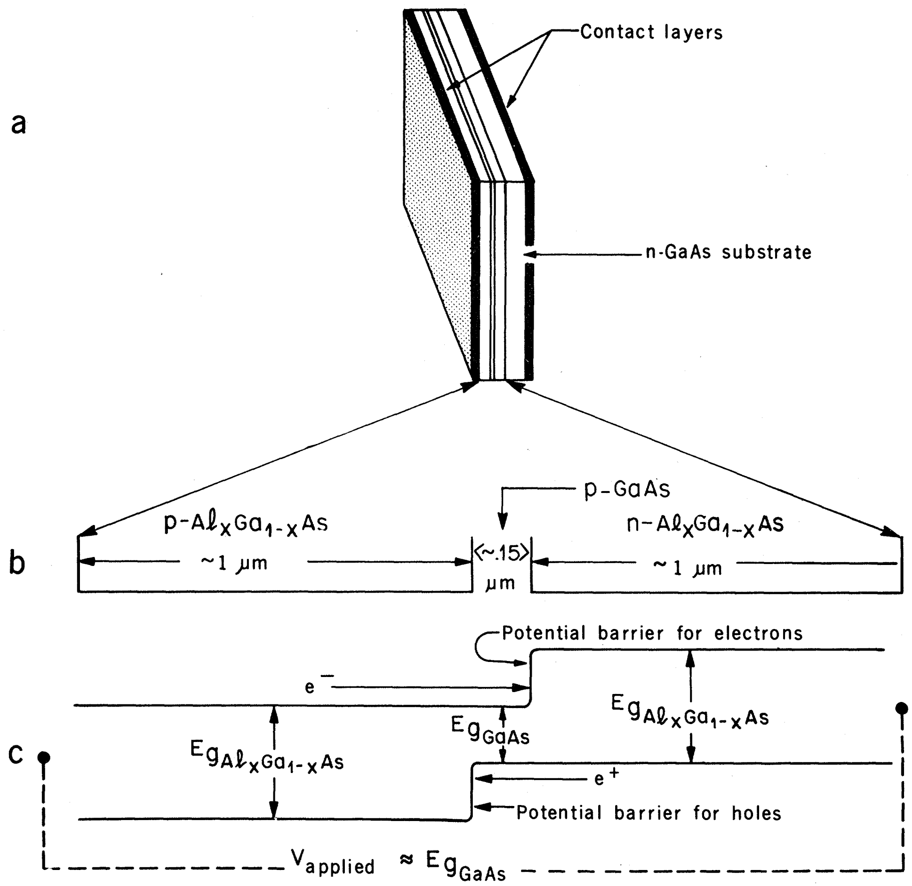

Fig. 4. (a) A double-heterostructure laser. (b) The epitaxial layers. (c) Conduction and valence band edges under forward bias from an applied voltage $V_{applied} \approx E_{g_{GaAs}}$.

only the devices mentioned above but also optical detector and microwave devices such as field-effect transistors, all on a single semiconductor chip. The MBE technique may be particularly useful for such complex structures because it permits lateral dimensional control by means of shadow masking. Studies of shadow masking during MBE (*30*) are illustrated in Fig. 5a, which shows how mesas and tapers are grown. A three-layer mesa is shown in Fig. 5b. A similar technique has already been used to prepare a laser-taper coupler combination (*31*).

Monolayers and Quantum Wells

Given the ability to obtain extremely smooth surfaces, a slow and precise growth rate, controlled impurity incorporation as a function of depth, and composition variation as a function of depth, several workers have elected to study a range of multilayered structures with extraordinarily small dimensions in layer thickness. The structures with the thinnest layers are the so-called monolayer structures described by Gossard *et al.* (*32*).

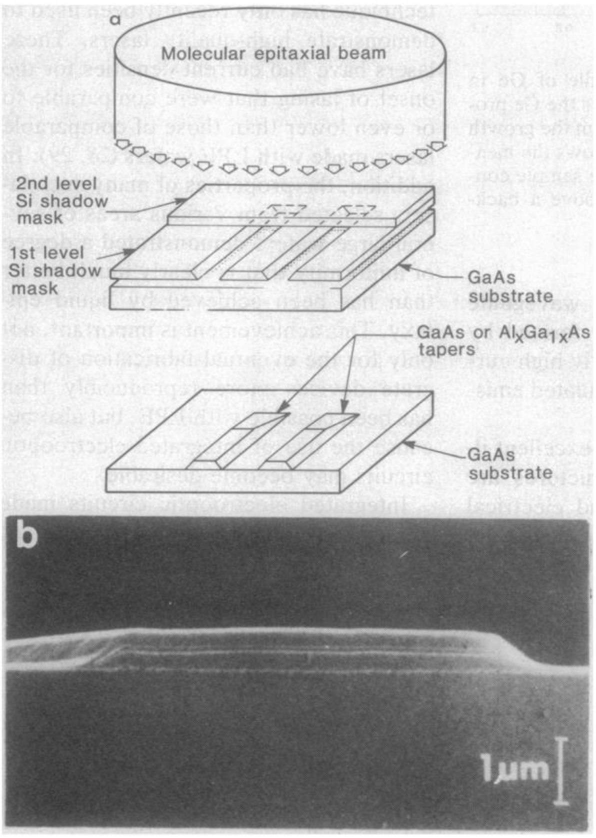

Fig. 5. (a) Schematic representation of shadow masking with MBE. (b) Cross section of a three-layer mesa grown by MBE through a shadow mask (*30*).

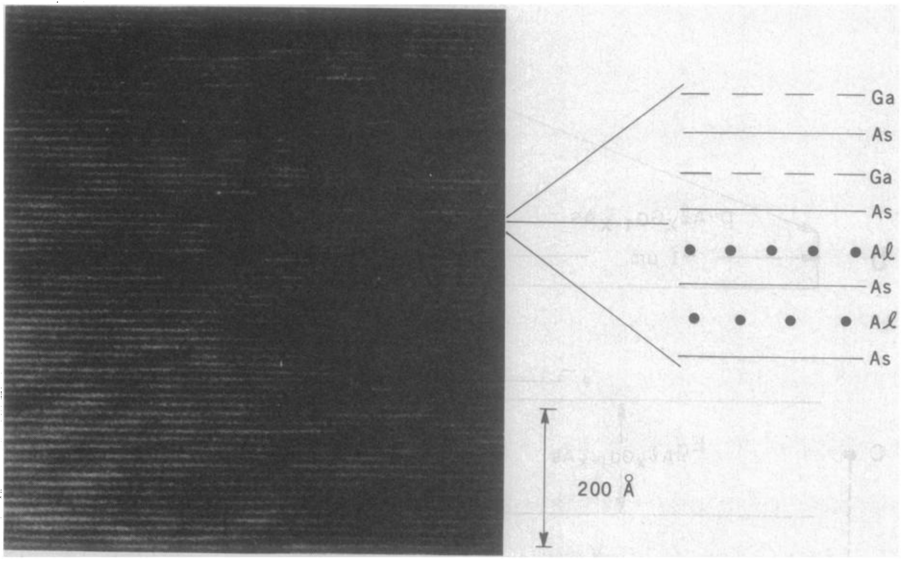

Fig. 6. Cross-sectional transmission electron micrograph of a "monolayer structure" consisting of interleaved bilayers nominally of GaAs and AlAs. The layer interfaces are in the 100 plane. [Micrograph provided by P. M. Petroff]

An approach to the ultimate in such single-crystal structures is illustrated in Fig. 6, which is a cross-sectional transmission electron micrograph of a stack of alternating GaAs and AlAs layers. To visualize the scale of these individual layers, the GaAs or AlAs crystal is shown schematically as a stack of alternating planes of gallium (or aluminum) and arsenic atoms. For the structure shown in Fig. 6, referred to as an alternate bilayer structure, each dark or light band consists of four atomic planes, two mostly of gallium atoms or mostly of aluminum atoms, interleaved with two planes of arsenic atoms, as illustrated on the right in Fig. 6. The group III element layers are, to some degree, mixtures of Al and Ga, hence the terms mostly Ga and mostly Al. Each nominally GaAs or AlAs layer is 5.6 Å thick, and stacks of such layers that are 10,000 Å thick have been grown on GaAs substrates. Stacks of alternating GaAs and AlAs layers consisting of single 2.8-Å monolayers were also grown and, in x-ray and electron diffraction, have shown the alternate single-monolayer composition. All these structures are new crystals that have periodicities not available in nature. They are grown by maintaining an unvarying arsenic beam on the substrate while alternately exposing it to the Ga and Al beams with precisely timed opening and closing of shutters interposed between the effusion ovens and the wafer. So far, such structures have been used to provide microscopic information on the MBE crystal growth process, to demonstrate the limits in dimensional precision of the MBE technique, and to correlate structural and physical properties of crystals in the limit of atomic dimensions.

Quantum well structures consist of somewhat thicker alternating layers of GaAs and, in this case, Al$_x$Ga$_{1-x}$As, with each layer in the range of 50 to ~ 400 Å thick. One such heterostructure is illustrated in Fig. 7a. The band edge energy diagram corresponding to the structure of Fig. 7a is illustrated schematically in Fig. 7b. The important characteristic of these structures is that the steps in the conduction and valence band edges at the heterojunctions form the boundaries of potential wells for electrons in the conduction band and holes in the valence band. When such quantum wells are present they can modify the macroscopic properties of the components of multilayer structures so that they differ from the equivalent properties of the bulk semiconductor. Keldysh (*33*) predicted effects due to quantization of carriers in artificial periodic potential structures in 1963. Esaki and Tsu (*34*) suggested in 1970 that such a structure, which they called a superlattice, would result from a one-dimensional periodic variation of solid solution composition in a III-V semiconductor. Particularly striking examples of the effects of quantum wells on properties of MBE layers of GaAs and $Al_xGa_{1-x}As$ have been demonstrated with optical absorption and electron mobility.

The individual quantum well is essentially a one-dimensional container for electrons, and quantum theory requires that for a sufficiently small container the electron moving in the confining direction can have only fixed energies. Thus, the quantum wells of Fig. 7a contain sets of energy subbands—the dashed lines in Fig. 7b—for electrons. Such "confined carrier quantum states" are clearly observable by optical absorption in GaAs quantum wells less than about 400 Å thick.

Bulk GaAs is essentially transparent to light of energy less than that of the width of the forbidden energy gap of GaAs (0.9 μm), but is strongly absorbing for light of higher energy because the higher energy photons are absorbed in the excitation of electrons from the valence band into the conduction band. This is illustrated in the top curve of Fig. 8, which shows the absorption spectrum of a 4000-Å-thick GaAs layer. The peak at the leading edge represents absorption by electrons that are excited into the conduction band, but are still bound by the Coulomb interaction to the holes in the valence band (exciton effects). When light is passed through a quantum well layer of GaAs the absorption of photons results from excitation of electrons from energy subbands in the valence band quantum well to subbands in the conduction band quantum well. These transitions occur at energies greater than the bulk GaAs band gap and provide the major optical absorption mechanism. As a result, the absorption spectrum of the quantum well shows bands characteristic of such transitions. These are illustrated in the bottom three curves in Fig. 8. Dingle *et al.* (*35*) showed that the transition energies can be quite accurately predicted with the well-known particle-in-a-box quantum theory calculation.

The structures used to obtain absorption data such as those shown in Fig. 8 are stacks of GaAs quantum wells with 20 or more GaAs layers. The substrate has been removed by chemical etching. Since the measurements are usually made by passing light through the structure in a direction orthogonal to the layer surface, the large number of GaAs layers is needed to provide sufficient material thickness for a useful absorption measurement. For these measurements the

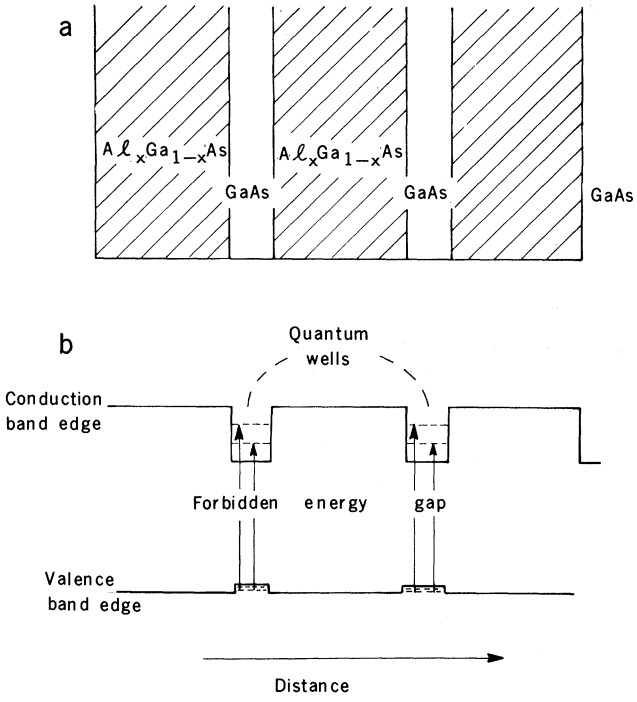

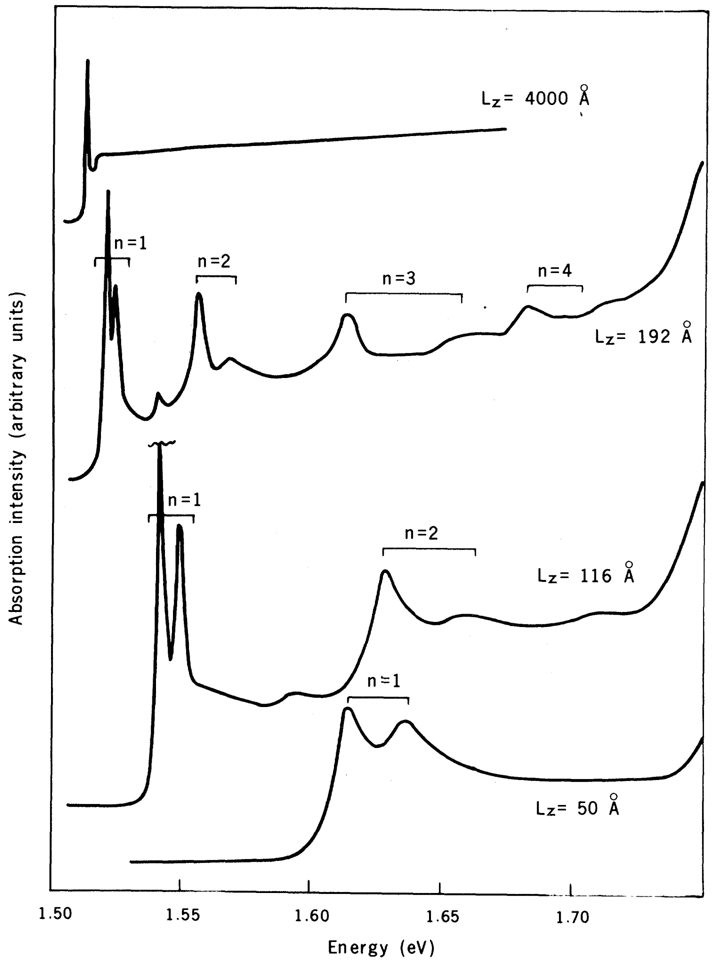

Fig. 7 (left). Schematic representation of (a) a cross section of a GaAs-$Al_xGa_{1-x}As$ quantum well structure and (b) band edges in the quantum structure of (a). Fig. 8 (right). Absorption spectra of GaAs layers 4000, 192, 116, and 50 Å thick between $Al_xGa_{1-x}As$ barriers. The quantum well structures consist of a sufficient number of GaAs layers to yield approximately the same absorption as the single GaAs layer used for the upper curve. The peaking at the transition energies is the result of exciton effects. Otherwise, the quantum well subbands would have given a more stepped absorption spectrum. The splitting of the various levels, *n*, results from the resolution of quantized levels in the hole quantum well. [Figure provided by R. Dingle] energy range of the light used is varied between that of the GaAs band gap and that of the $Al_xGa_{1-x}As$ band gap. Since the energy of the levels within the quantum well depends on its depth and width, both the Al content and the layer thickness must be highly reproducible for the absorption measurements to yield well-resolved data for the transition energies. In Fig. 8 the transitions from the confined hole subbands are clearly resolved. This requires a layer-to-layer reproducibility in thickness of less than 5 Å, a dramatic illustration of the precision in dimensional reproducibility that MBE permits. Large-angle x-ray studies of quantum well structures grown both at IBM (*36*) and at Bell Laboratories (*37*) have confirmed that the individual layers are flat and uniform with abrupt interfaces in which the entire composition change is achieved within 5 Å in the growth direction.

The possibility of modifying the transport characteristics of electrical carriers in the material comprising a quantum well results from the ability of the quantum well structure to provide a separation in space between the part of the structure occupied by dopant elements and the carriers they contribute to the semiconductor. The mobility of carriers in semiconductors is affected by many factors, including scattering by the ionized impurity atoms that donated the electrons in the first place. If, during the MBE growth of a quantum well structure, donor atoms are added to the $Al_xGa_{1-x}As$ layer but not to the GaAs layer, the electrons in the conduction band, which seek the lowest possible energy states, fall into the GaAs quantum well. They then occupy quantum well energy subbands. Thus it is possible, by using MBE to grow such "modulated-doping" quantum well structures (*38*), to have GaAs that contains donated electrons without having the donor atoms present in the semiconducting layer. The reduction in scattering by impurity atoms is reflected in the greater mobility of the electrons in the quantum well material than in equivalent doped bulk GaAs.

The MBE-grown quantum well structures and other heterostructures that require extremely thin epitaxial layers are under investigation from a number of different points of view. Heterostructure lasers that incorporate several quantum wells in the center (active) layer have better longitudinal mode stability and a smaller temperature dependence of threshold current than the equivalent more conventional structures (*39*). The higher mobility of electrons in GaAs modulated-doping quantum wells has led to studies, now under way, of the possibility for improvement in the speed of GaAs microwave devices. Quantum well structures have also been used to investigate the fundamental properties of the two-dimensional electron gas (*40, 41*), the possibility of fabricating energy-selective phonon mirrors (*42*), and, in InAs-GaSb structures, the creation of artificial semimetals (*13*). In addition, $GaAs\text{-}Al_xGa_{1-x}GaAs$ heterostructures in which the $Al_xGa_{1-x}As$ layer is very thin (≤ 500 Å) and has a graded band gap obtained by varying x have been shown to form very simple current rectifiers that should be totally compatible with other optical or electronic devices that may be integrated onto the same chip (*43*).

Conclusion

A rather brief and general description of some of the developments in molecular beam epitaxy, using only the semiconductors GaAs and $Al_xGa_{1-x}As$ as prototypes, has been presented. Because it is possible to maintain high semiconductor quality at very low growth rates, MBE permits extensive dimensional control in epitaxial layer thickness and dopant element profiles. Unlike other crystal growth methods, it also permits growth of complex epitaxial structures with controlled lateral dimensions because of the possibility for shadow masking. These developments have resulted in a burgeoning of MBE studies of fundamental properties of very thin structures and of the use of MBE for optoelectronic and microwave devices.

References and Notes

1. K. G. Günther, *Naturwissenschaften* **45**, 415 (1958).
2. ———, in *Compound Semiconductors*, R. K. Willardson and H. L. Goering, Eds. (Reinhold, New York, 1961), vol. 1, p. 313.
3. R. F. Steinberg and D. M. Scruggs, *J. Appl. Phys.* **37**, 4586 (1966).
4. J. E. Davey and T. Pankey, *ibid.* **39**, 1941 (1968).
5. J. R. Arthur, *ibid.*, p. 4032.
6. A. Y. Cho and J. R. Arthur, *Prog. Solid State Chem.* **10**, 157 (1975).
7. A. Y. Cho, *J. Vac. Sci. Technol.* **16**, 275 (1979).
8. L. L. Chang and R. Ludeke, in *Epitaxial Growth*, J. W. Mathews, Ed. (Academic Press, New York, 1975), part A, p. 37.
9. K. Ploog, in *Crystal Growth, Properties and Applications*, L. F. Boschke, Ed. (Springer-Verlag, Heidelberg, 1979).
10. R. C. Farrow, *J. Phys. D* **7**, 121 (1974).
11. J. H. Miller, B. I. Miller, K. M. Bachmann, *J. Electrochem. Soc.* **124**, 259 (1977).
12. B. I. Miller and J. H. McFee, *ibid.* **125**, 1311 (1978).
13. L. L. Chang, G. A. Sai-Halsz, N. J. Kawai, I. Esaki, *J. Vac. Sci. Technol.* **16**, 1504 (1979).
14. Y. Ota, *J. Electrochem. Soc.* **124**, 1795 (1977).
15. G. E. Becker and J. C. Bean, *J. Appl. Phys.* **48**, 3395 (1977).
16. J. C. Bean, *Appl. Phys. Lett.* **36**, 741 (1980).
17. H. Holloway and J. N. Walpole, in *Progress in Crystal Growth and Characterization*, B. R. Pamplin, Ed. (Pergamon, New York, 1979), vol. 2, pp. 49–94.
18. A. Y. Cho, *J. Vac. Sci. Technol.* **8**, S31 (1971).
19. ———, *J. Appl. Phys.* **46**, 1733 (1975).
20. ——— and F. K. Reinhart, *ibid.* **45**, 1812 (1974).
21. A. Y. Cho, C. N. Dunn, R. L. Kuvas, W. E. Schroeder, *Appl. Phys. Lett.* **25**, 224 (1974).
22. S. G. Bandy, D. M. Collins, C. K. Nishimoto, *Electron. Lett.* **15**, 218 (1979).
23. M. V. Schneider, R. A. Linke, A. Y. Cho, *Appl. Phys. Lett.* **31**, 219 (1977).
24. J. V. DiLorenzo, W. C. Niehaus, A. Y. Cho, *J. Appl. Phys.* **50**, 951 (1979).
25. W. T. Tsang, *Appl. Phys. Lett.* **33**, 426 (1978).
26. H. C. Casey, Jr., A. Y. Cho, P. W. Foy, *ibid.* **34**, 594 (1979).
27. H. C. Casey, Jr., and M. B. Panish, *Heterostructure Lasers* (Academic Press, New York, 1978).
28. W. T. Tsang, *Appl. Phys. Lett.* **34**, 473 (1979).
29. A. Y. Cho, H. C. Casey, Jr., C. Radice, P. W. Foy, *Electron. Lett.* **16** (No. 2), 72 (1980).
30. W. T. Tsang and M. Ilegems, *Appl. Phys. Lett.* **31**, 301 (1977).
31. F. K. Reinhart and A. Y. Cho, *ibid.*, p. 457.
32. A. C. Gossard, P. M. Petroff, W. Wiegmann, R. Dingle, *ibid.* **29**, 323 (1976).
33. L. V. Keldysh, *Sov. Phys. Solid State* **4**, 1658 (1963).
34. L. Esaki and R. Tsu, *IBM J. Res. Dev.* **14**, 61 (1970).
35. R. Dingle, W. Wiegmann, C. H. Henry, *Phys. Rev. Lett.* **33**, 827 (1974).
36. L. L. Chang, A. Segmuller, L. Esaki, *Appl. Phys. Lett.* **28**, 39 (1976).
37. R. M. Fleming *et al.*, *J. Appl. Phys.* **51**, 357 (1980).
38. R. Dingle, H. L. Störmer, A. C. Gossard, W. Wiegmann, *Appl. Phys. Lett.* **33**, 665 (1978).
39. W. T. Tsang, C. Weisbuch, R. C. Miller, R. Dingle, *ibid.* **35**, 673 (1979).
40. D. C. Tsui, H. Störmer, A. C. Gossard, W. Wiegmann, *Phys. Rev B* **21**, 1589 (1980).
41. L. L. Chang, H. Sakaki, C. H. Change, L. Esaki, *Phys. Rev. Lett.* **38**, 1489 (1977).
42. V. Narayanamurti, H. L. Störmer, M. A. Chin, A. C. Gossard, W. Wiegmann, *ibid.* **43**, 2012 (1979).
43. C. L. Allyn, A. C. Gossard, W. Wiegmann, *Appl. Phys. Lett.* **36**, 373 (1980).
44. W. T. Tsang and M. Ilegems, *ibid.* **35**, 792 (1979).